

## UV Photodissociation of Matrix-Isolated Propionyl Chloride

Paul R. Winter,<sup>†</sup> Brad Rowland,<sup>‡</sup> Wayne P. Hess,<sup>‡</sup> Juliusz G. Radziszewski,<sup>§</sup>  
Mark. R. Nimlos,<sup>§</sup> and G. Barney Ellison<sup>\*,†</sup>

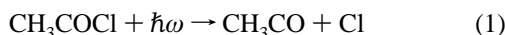
Department of Chemistry & Biochemistry, University of Colorado, Boulder, Colorado 80309-0215, Environmental Molecular Sciences Laboratory, Pacific Northwest National Laboratory, P.O. Box 999, Richland, Washington 99352, and National Renewable Energy Laboratory, 1617 Cole Boulevard, Golden, Colorado 80401

Received: November 21, 1997; In Final Form: February 11, 1998

We have investigated the photodecomposition of propionyl chloride,  $\text{CH}_3\text{CH}_2\text{COCl}$ , in an argon matrix at 10 K using FTIR absorption spectroscopy. The decomposition products formed following irradiation at 266, 254, or 248 nm are methyl ketene,  $\text{CH}_3\text{CH}=\text{CO}$ , and HCl; no other photoproducts are observed. We have carried out FTIR polarization studies to determine the relative orientation of the photoproducts and found that the HCl molecule is situated perpendicular to the carbonyl group in the methyl ketene. The orientation in the photoproducts and kinetic studies of the acid chloride dissociation point to a direct elimination mechanism for propionyl chloride decomposition. This is consistent with the direct mechanism proposed for acetyl chloride,  $\text{CH}_3\text{COCl}$ , photodissociation in both an argon matrix and the solid crystalline form. We have calculated detailed thermodynamics for  $\text{CH}_3\text{COCl}$  and  $\text{CH}_3\text{CH}_2\text{COCl}$  decomposition and found them consistent with the proposed elimination mechanism. We also assign the fundamental vibrational frequencies for the methyl ketene–HCl complex on the basis of ab initio calculations and polarization studies.

### 1. Introduction

The UV photodissociation of the most elementary acid chloride, acetyl chloride ( $\text{CH}_3\text{COCl}$ ), has been previously studied in both the gas and solid phases.<sup>1–8</sup> The photoproducts are found to depend on the initial phase of the reactant. In the gas phase, UV excitation of  $\text{CH}_3\text{COCl}$  at 236 nm results in cleavage of the C–Cl bond and the formation of Cl and  $\text{CH}_3\text{CO}$  as the primary products; the acetyl radical then may fragment further.



The first step (1) produces a chlorine atom and a rotationally vibrationally excited acetyl radical in less than 1 ps.<sup>4,8</sup> This radical decomposes to form carbon monoxide and methyl radical (2) on a slower time scale. The initial dissociation of the C–Cl bond is known to take place entirely on an excited singlet potential surface.<sup>7,8</sup>

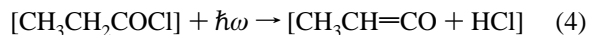
In an Ar matrix, however, irradiation of  $\text{CH}_3\text{COCl}$  at 266, 254, or 248 nm leads to an elimination reaction forming ketene,  $\text{CH}_2\text{CO}$ , and HCl.



(Brackets will be used throughout this paper to indicate reactions in the condensed phase.) These products are also the only products observed upon irradiation of neat crystalline and amorphous samples of acetyl chloride.<sup>2</sup> Following the HCl elimination, the  $\text{CH}_2\text{CO}$  and HCl molecules are trapped as a

dimer complex in the solid matrix at 10 K.<sup>2,3</sup> The reaction in both the argon matrix and the neat solid is thought<sup>1,2</sup> to proceed through a direct elimination mechanism rather than through C–Cl bond dissociation.

To further understand the mechanism for the condensed-phase photodecomposition of acid chlorides, we have used FTIR absorption spectroscopy to probe the photodecomposition products of propionyl chloride,  $\text{CH}_3\text{CH}_2\text{COCl}$ , in an Ar matrix at 10 K following irradiation at 248, 254, and 266 nm. The observed products are methyl ketene and hydrochloric acid (4).



These products are analogous to those observed in condensed-phase photodissociation of  $\text{CH}_3\text{COCl}$ . No other products are observed, even after prolonged irradiation of  $\text{CH}_3\text{CH}_2\text{COCl}$ . We have assigned the vibrational modes for propionyl chloride in Ar and for the product methyl ketene/HCl complex. These assignments were verified by ab initio calculations of the methyl ketene and propionyl chloride vibrational frequencies. Polarization FTIR studies were conducted to determine the orientation of the photoproducts, and they show that the HCl is oriented perpendicular to the  $\text{C}=\text{C}=\text{O}$  structure in methyl ketene. The presence of orientated HCl in the photoproducts of (4) suggests that the reaction does not proceed via hydrogen abstraction by a free chlorine atom but rather through a direct elimination process. This mechanism is supported by the thermochemistry of propionyl and acetyl chloride dissociation.

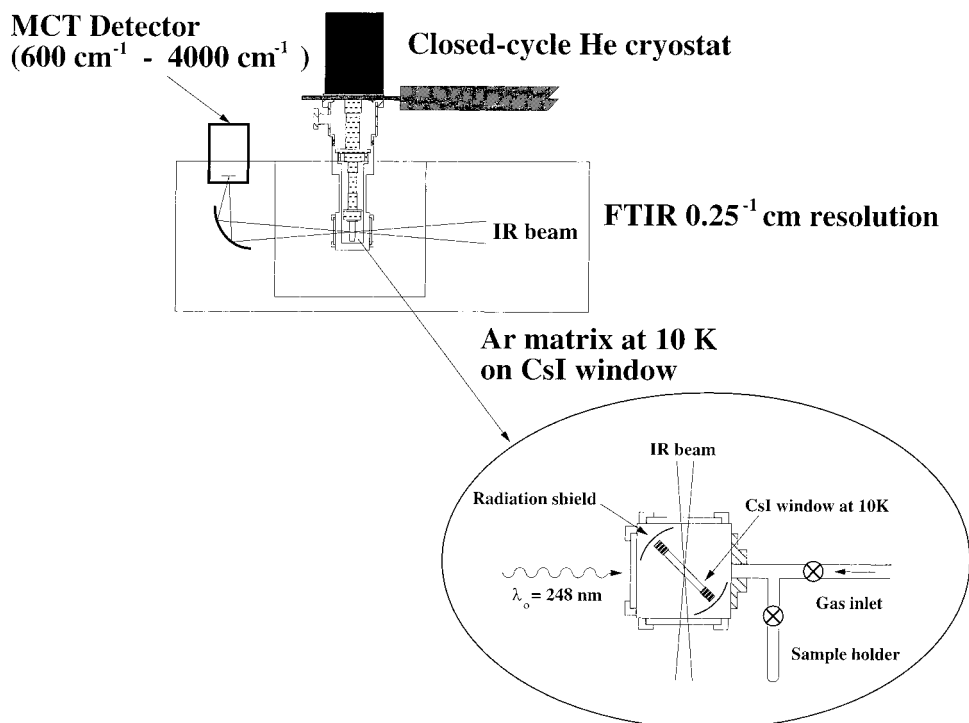
### 2. Experimental Section

The experimental apparatus is shown in Figure 1. Propionyl chloride (98%) was purchased from Aldrich; several freeze–pump–thaw cycles were conducted before the initial deposition

<sup>†</sup> University of Colorado.

<sup>‡</sup> Pacific Northwest National Laboratory.

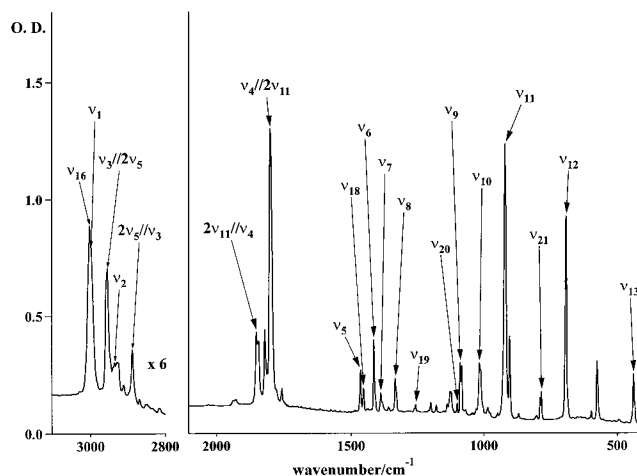
<sup>§</sup> National Renewable Energy Laboratory.



**Figure 1.** Overview of experimental apparatus. The inset shows the arrangement allowing UV irradiation while simultaneously recording an IR spectrum.

to purify the sample.  $\text{CH}_3\text{CH}_2\text{COCl}$  vapor was mixed with argon gas in amounts ranging from 0.25% to 0.65%. These mixtures were deposited at flow rates between  $1 \times 10^{-6}$  and  $3 \times 10^{-6}$  mol/min for about 30 min on a CsI window, which was held at a temperature of 30 K during the deposition and then cooled to 10 K after the deposition was completed. After an initial IR spectrum was recorded, the matrix was irradiated with 254-nm photons from one or two mercury vapor lamps or 248-nm photons from an excimer laser at around 10 mJ, 20 Hz. The UV irradiation was incident at a  $45^\circ$  angle to the CsI window, and the infrared radiation from the FTIR was passed through the matrix perpendicular to the UV irradiation (Figure 1, inset) allowing spectra to be collected while simultaneously irradiating without moving the matrix. Spectra were collected at regular intervals during the irradiation until the propionyl chloride peaks were no longer observed. A spectrum of the products was obtained by subtracting the initial spectrum from the final spectrum; the product bands appear as positive features and the precursor bands as negative features in the difference spectrum. This spectrum was then analyzed to identify the irradiation products. The intermediate spectra were used to monitor the decay and growth kinetics of the precursor and product features, respectively.

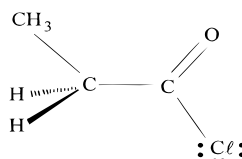
The polarization studies were conducted using a previously described<sup>2</sup> apparatus. A propionyl chloride/Ar gas mixture (0.2–0.4%) was deposited onto a CsI window at 11 K until the matrix was about  $5\text{--}6 \mu\text{m}$  thick. The irradiation was accomplished using linearly polarized 266-nm light from the fourth harmonic of a Nd:YAG laser at 5 mJ, 20 Hz. The sample was irradiated until approximately 20% of the precursor was decomposed, producing a suitable amount of photooriented product for detection. Polarization FTIR spectra of the products were collected at various angles with respect to the polarization of the UV irradiation.



**Figure 2.** IR absorption spectrum of propionyl chloride,  $\text{CH}_3\text{CH}_2\text{COCl}$ , in an argon matrix at 10 K.

### 3. Results

**Propionyl Chloride and Methyl Ketene Spectra.** The IR absorption spectrum of  $\text{CH}_3\text{CH}_2\text{COCl}$  in an Ar matrix is shown in Figure 2 with the fundamentals assigned (Table 1). Our assignments are based on literature assignments in the gas and solid phases<sup>9</sup> and were checked by comparison with spectra of  $\text{CH}_3\text{CH}_2\text{COCl}$  vapor at 1.7 Torr in a 10-cm cell. IR spectra of the matrix before and after irradiation at 266 nm are shown in Figure 3. The  $\text{CH}_3\text{CH}_2\text{COCl}$  peaks are almost totally absent following 2 h irradiation with 5 mJ, 20 Hz at 266 nm. The duration of the irradiation in these experiments varied from several hours to overnight, depending on the initial matrix, but in all cases near complete decomposition could be achieved. Longer irradiation (including up to several days at 254 nm) resulted in no further change.

**TABLE 1: Vibrational Modes of Propionyl Chloride**

species	mode	gas phase <sup>9</sup>	Ar matrix <sup>this work</sup>	(unscaled) ab initio harmonic frequencies and intensities DFT calc: B3LYP/cc-pVDZ		
				$\omega/\text{cm}^{-1}$	$A/\text{km mol}^{-1}$	local mode
a'	$\nu_1$	2981	3003	3127	13.7	sym CH <sub>3</sub> stretch
	$\nu_2$	2941	2947	3050	4.5	sym CH stretch "in phase"
	$\nu_3$	2930	2960 <sup>a</sup>	3049	18.6	sym CH stretch "out of phase"
	$\nu_4$	1830	1803 <sup>b</sup>	1900	285.7	C=O stretch
	$\nu_5$	1472	1465	1474	7.4	CH <sub>3</sub> scissors
	$\nu_6$	1421	1416	1423	14.6	CH <sub>2</sub> scissors
	$\nu_7$	1385	1389	1401	5.1	CH <sub>3</sub> umbrella
	$\nu_8$	1339	1334	1348	8.7	CH <sub>2</sub> wag
	$\nu_9$	1084	1090	1099	26.4	CH <sub>3</sub> wag
	$\nu_{10}$	1016	1018	1018	29.4	asym C-C-C stretch
	$\nu_{11}$	926	923	926	174.7	sym C-C-C stretch
	$\nu_{12}$	697	696	693	98.0	C-C-C-O bend
	$\nu_{13}$	441	437	423	18.4	C-Cl stretch
	$\nu_{14}$	359		353	27.2	C-C-Cl bend
a''	$\nu_{15}$	229		225	2.3	CH <sub>3</sub> rock
	$\nu_{16}$	2999	3007	3130	14.9	asym CH <sub>3</sub> stretch
	$\nu_{17}$	2930 <sup>c</sup>		3081	0.6	asym CH <sub>2</sub> stretch
	$\nu_{18}$	1456	1454	1464	7.3	CH <sub>3</sub> bending
	$\nu_{19}$	1261	1262	1265	0.1	CH <sub>2</sub> rock
	$\nu_{20}$	1088	1085	1085	0.1	CH <sub>3</sub> rock
	$\nu_{21}$	788	791	790	8.2	
	$\nu_{22}$	505	494	497	0.7	
	$\nu_{23}$	196 <sup>d</sup>	212		0.7	CH <sub>3</sub> torsional
	$\nu_{24}$	71 <sup>d</sup>	77		0.9	CH <sub>3</sub> -CH <sub>2</sub> torsion

<sup>a</sup> Value for  $\nu_3$  Fermi resonance with  $2\nu_5$ . The other resonance peak is at  $2889.2 \text{ cm}^{-1}$ . <sup>b</sup> Value for  $\nu_4$  Fermi resonance with  $2\nu_{11}$ . The other resonance peak is at  $1851.9 \text{ cm}^{-1}$ . <sup>c</sup> Value determined from Raman absorption in the condensed phase. <sup>d</sup> Value determined from IR combination tone.

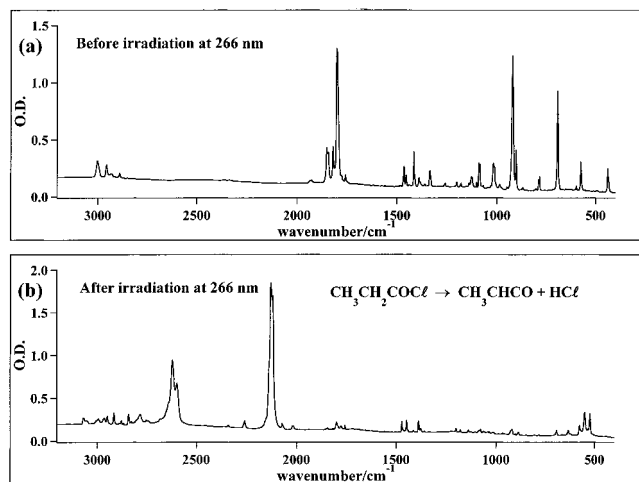


**Figure 3.** IR absorption spectra of (a) propionyl chloride in an Ar matrix before irradiation and (b) the product matrix following irradiation at 266 nm.

All of the trials showed the strongest product peak at  $2130 \text{ cm}^{-1}$ , close to the value of  $2125 \text{ cm}^{-1}$  reported<sup>10,11</sup> for the carbonyl stretch of  $\text{CH}_3\text{CH}=\text{O}$  in an Ar matrix. All of the trials also contained a broad doublet at  $2597$  and  $2619 \text{ cm}^{-1}$ . We attribute this feature to HCl in a  $[\text{CH}_3\text{CH}=\text{C}=\text{O}, \text{HCl}]$  complex; an analogous  $[\text{CH}_2=\text{C}=\text{O}, \text{HCl}]$  complex was observed<sup>2,3</sup> at  $2679 \text{ cm}^{-1}$  in the acetyl chloride photoproducts, red-shifted from the isolated HCl monomer in an Ar matrix at  $2860 \text{ cm}^{-1}$ . Numerous other features were also consistently evident in the product spectrum. The difference spectrum following

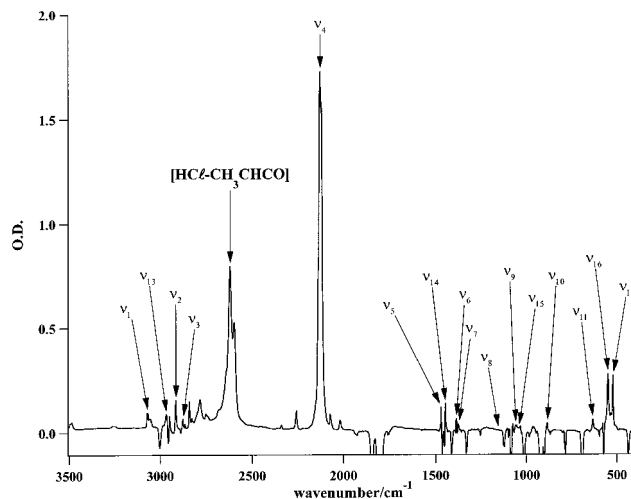


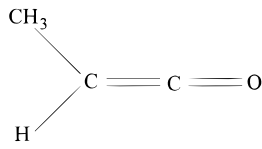
**Figure 4.** Difference spectrum showing the product features as positive peaks and precursor features as negative peaks. The main features for methyl ketene,  $\text{CH}_3\text{CHCO}$ , are labeled, along with the feature attributed to the  $[\text{HCl}-\text{CH}_3\text{CHCO}]$  complex.

$254 \text{ nm}$  irradiation of  $\text{CH}_3\text{CH}_2\text{COCl}$  is shown in Figure 4. The fundamental bands for methyl ketene have been assigned on the basis of the partial assignments of Harrison and Frei<sup>11</sup> for methyl ketene in an Ar matrix and our ab initio electronic structure calculations.

A B3LYP/cc-pVDZ electronic structure calculation was carried out using the Gaussian 94 Suite of codes<sup>12</sup> to determine the geometry and identify the harmonic frequencies of methyl

TABLE 2: Vibrational Modes of Methyl Ketene

$\text{CH}_3\text{CH}=\text{C}=\text{O}$



		(unscaled) ab initio harmonic frequencies and intensities DFT calc: B3LYP/cc-pVDZ				
	mode	Ar matrix <sup>this work</sup>	Ar matrix <sup>11</sup>	$\omega/\text{cm}^{-1}$	$A/\text{km mol}^{-1}$	local mode
a'	$\nu_1$	3069		3182 <sup>a</sup>	6.3	C–H stretch
	$\nu_2$	2916		3117 <sup>a</sup>	16.4	sym CH <sub>3</sub> stretch “out of phase”
	$\nu_3$	2878	2912.1	3022 <sup>a</sup>	42.2	sym CH <sub>3</sub> stretch “in phase”
	$\nu_4$	2130	2125.2	2216	619.3	C=C=O stretch
	$\nu_5$	1471	1470.7	1484	3.6	
	$\nu_6$	1388		1397 <sup>b</sup>	16.4	CH <sub>3</sub> umbrella
	$\nu_7$	1376		1408 <sup>b</sup>	2.4	
	$\nu_8$	1155		1145	0.6	CCH bend
	$\nu_9$	1063	1075.5	1076	9.3	
	$\nu_{10}$	886		902	3.2	CH <sub>3</sub> wag
	$\nu_{11}$	634		645	5.8	CCO bend
	$\nu_{12}$			209	1.8	CCC bend
a''	$\nu_{13}$	2966		3077 <sup>a</sup>	23.1	asym CH <sub>3</sub> stretch
	$\nu_{14}$	1447	1447.3	1453	5.1	
	$\nu_{15}$	1043		1042	0.1	CH <sub>3</sub> rock
	$\nu_{16}$	551		540	46.5	O–C–C–H bend
	$\nu_{17}$	523	521	517	13.5	CH bend
	$\nu_{18}$			149	0.1	CH <sub>3</sub> torsional motion

<sup>a</sup> In the IR spectrum of the partially deuterated CH<sub>3</sub>CD<sub>2</sub>CO, the feature at 3069 cm<sup>-1</sup> is completely absent; for this reason, it is assigned as  $\nu_1$ . The features at 2916 and 2878 cm<sup>-1</sup> are found to be a' modes by the polarization analysis, so they are assigned as  $\nu_2$  and  $\nu_3$ . This leaves the feature at 2966 cm<sup>-1</sup> as  $\nu_{13}$ ; owing to overlap with  $\nu_3$  of the precursor propionyl chloride, it was not possible to verify the symmetry of this mode. <sup>b</sup>  $\nu_6$  shows no shift upon deuteration, as expected for the CH<sub>3</sub> umbrella mode, while  $\nu_7$  shifts by approximately 2 cm<sup>-1</sup> upon deuteration.

TABLE 3: Vibrational Modes of Ketene, H<sub>2</sub>C=C=O

		(unscaled) ab initio harmonic frequencies and intensities DFT calc: B3LYP/cc-pVDZ				
	mode	gas phase <sup>43</sup>	Ar matrix <sup>44</sup>	$\omega/\text{cm}^{-1}$	$A/\text{km mol}^{-1}$	local mode
a <sub>1</sub>	$\nu_1$	3070	3062	3182	28.5	C–H sym str.
	$\nu_2$	2153	2142	2229	564.7	C=O (asym) str.
	$\nu_3$	1387	1381	1389	14.1	CH <sub>2</sub> scissors
	$\nu_4$	1116	1115	1165	9.0	C=C (sym) str.
b <sub>1</sub>	$\nu_5$	587	591	582	25.8	CH <sub>2</sub> wag
	$\nu_6$	528	525	528	101.4	C=C=O linear bend
b <sub>2</sub>	$\nu_7$	3159	3155	3288	10.0	C–H asym str.
	$\nu_8$	978	974	975	6.5	CH <sub>2</sub> rock
	$\nu_9$	439	438	439	2.2	C=C=O linear bend

ketene (Table 2). A calculation of the same type was performed for ketene for the purposes of evaluating the accuracy of the methyl ketene calculation (Table 3). Our unscaled harmonic frequencies are within a few percent of the experimental values for both the methyl ketene and the ketene. On the basis of these calculations, a symmetry was assigned for each mode (CH<sub>3</sub>CH=C=O has C<sub>s</sub> symmetry). The polarization data and product spectra from the irradiation of CH<sub>3</sub>CD<sub>2</sub>COCl were used to confirm the assignments for these modes.

The UV absorption spectra of gas-phase acetyl and propionyl chloride are given in Figure 5. The gas-phase UV spectra of the two species are nearly identical in shape and intensity; both have a maximum at about 242 nm (5.1 eV). The UV spectra of the Ar matrix-isolated species are not significantly different from those in the gas phase.

**Absence of Other Products.** Thermodynamically, there are several available channels for propionyl chloride decomposition following excitation at 248 nm (115.3 kcal mol<sup>-1</sup>). The most stable channel leads to the formation of CH<sub>3</sub>CH<sub>2</sub>Cl and CO; other allowed channels lead to CH<sub>2</sub>=CH<sub>2</sub>, CO, and HCl ( $\beta$ -elimination/abstraction) or CH<sub>3</sub>CH=C=O and HCl ( $\alpha$ -elimina-

tion/abstraction). Figure 6 shows a comparison of the product spectrum with matrices of ethylene in argon and CO in argon. The strongest IR mode for ethylene<sup>13</sup> in an argon matrix is  $\nu_7$  at 946 cm<sup>-1</sup> (949 cm<sup>-1</sup> in the gas phase); there are also strong features at 1440 and 2995 cm<sup>-1</sup>. None of the product spectra contain features at these frequencies; therefore, CH<sub>2</sub>=CH<sub>2</sub> is not a photoproduct. Carbon monoxide absorbs at 2143 cm<sup>-1</sup> in an argon matrix. While this peak is close to the strong ketene C=C=O absorption, the two features are resolvable. None of the trials show any trace of CO produced during the photodecomposition. Ethyl chloride has strong gas-phase absorptions<sup>14</sup> at 3014, 2986, 1289, 974, and 677 cm<sup>-1</sup>; there are no features in the product spectrum that match these bands. The channels that lead to these products are not active despite being thermodynamically accessible.

Photolysis of the selectively deuterated species CH<sub>3</sub>CD<sub>2</sub>COCl was studied to search for HCl produced by a  $\beta$ -elimination/abstraction process. Irradiation at 254 nm produced only DCl as a product with no trace of either free HCl or the [CH<sub>3</sub>-CH=C=O, HCl] complex, thus confirming that only an  $\alpha$ -elimination/abstraction channel is active.

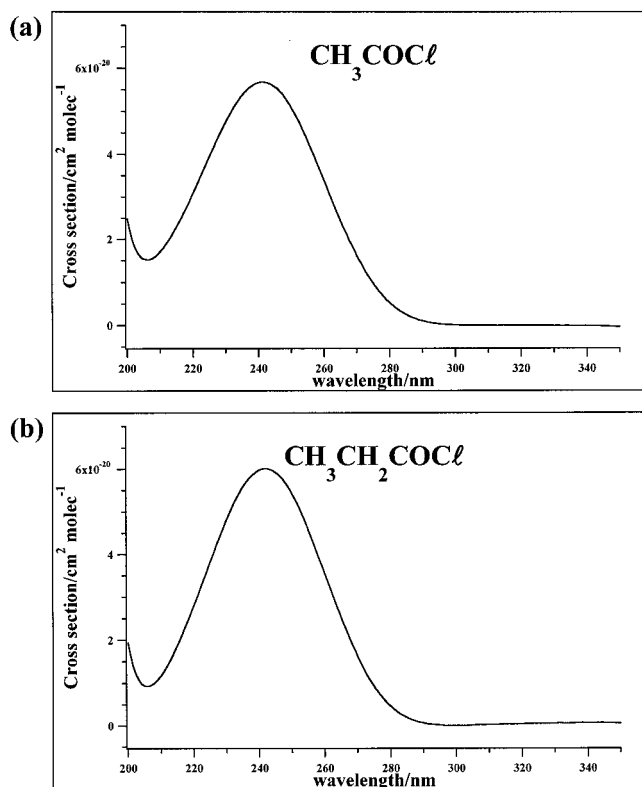


**Figure 5.** Gas-phase UV absorption spectra of (a) acetyl chloride,  $\text{CH}_3\text{COCl}$ , and (b) propionyl chloride,  $\text{CH}_3\text{CH}_2\text{COCl}$ .

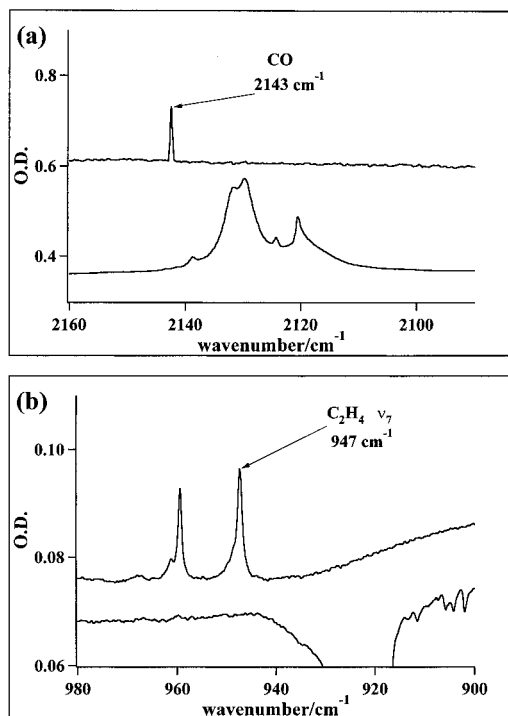


**Figure 6.** Comparison of the product spectrum with possible decomposition products. (a) shows CO in an Ar matrix at  $2143\text{ cm}^{-1}$  compared with the product spectrum, in which the  $\text{C}=\text{C}=\text{O}$  stretching mode is seen at  $2130\text{ cm}^{-1}$ . (b) shows a spectrum of ethylene in an Ar matrix, with a pair of peaks at  $947$  and  $958\text{ cm}^{-1}$ , compared with the product spectrum.

#### 4. Discussion

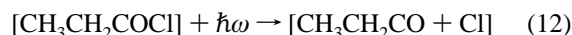
There are several conceptually different pathways by which an acid chloride could photodissociate in an Ar matrix: (I) a multistep process proceeding through a radical pair, with the

first step identical to the gas-phase fragmentation, followed by a radical–radical reaction, (II) a direct HCl elimination following the initial photoexcitation, or (III) fragmentation into an ion pair, followed by ion–ion chemistry. For  $\text{CH}_3\text{COCl}$ , all three of these mechanisms lead to HCl and  $\text{CH}_2\text{CO}$ , the observed photodecomposition products; only the radical–pair mechanism has a possible product channel other than that observed.  $\text{CH}_3\text{CH}_2\text{COCl}$ , on the other hand, has several different possible product channels for each proposed mechanism.

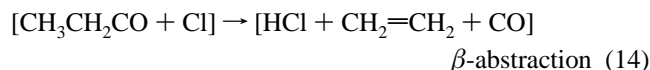
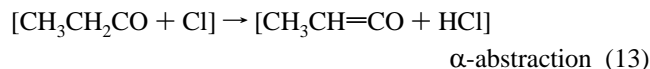
In the gas phase, propionyl chloride dissociates<sup>15</sup> to give chlorine atom and the propionyl radical,  $\text{CH}_3\text{CH}_2\text{CO}$ , following excitation at  $248\text{ nm}$ . Subsequent dissociation of the propionyl radical may be expected (10–11).



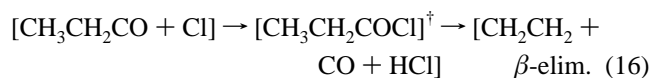
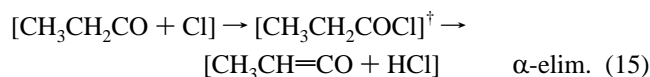
In a radical–radical process, I, if we assume the same initial fragmentation step as observed in the gas-phase following photoexcitation, the chlorine atom fragment will be trapped by the surrounding matrix (12).



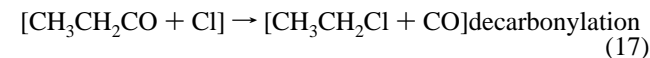
The resulting radical–radical chemistry could proceed along three lines: abstraction, recombination/elimination, or decarbonylation. The chlorine atom could abstract hydrogen from the propionyl radical at either the  $\alpha$ - or  $\beta$ -sites (13–14).



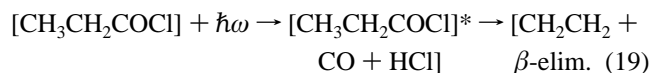
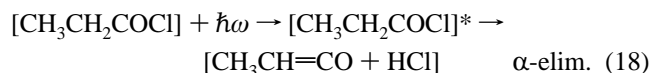
Alternatively, the chlorine atom could recombine with the propionyl radical and eliminate HCl on the electronic ground state (15, 16).



(We will use  $\ddagger$  to designate a rotationally/vibrationally excited, or “hot”, ground-state species.) Finally, the chlorine atom could react with the propionyl radical and produce carbon monoxide and ethyl chloride (17).



A direct elimination mechanism, II, will produce HCl and other products through an  $\alpha$ - or  $\beta$ -elimination (18–19).

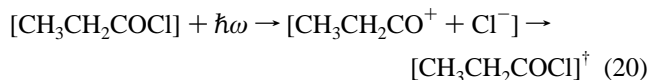


The first step of a reaction proceeding through an ion pair, III, would be fragmentation into  $\text{Cl}^-$  and  $\text{CH}_3\text{CH}_2\text{CO}^+$  ions. As

TABLE 4: Heats of Formation of Relevant Species

species	$\Delta_f H_0/\text{kcal mol}^{-1}$	$\Delta_f H_{298}/\text{kcal mol}^{-1}$	ref
CH <sub>3</sub> COCl	-55.9 ± 0.2	-58.0 ± 0.2	19, 20
CH <sub>3</sub> CO	-0.9 ± 0.3	-2.4 ± 0.3	45
Cl	28.590 ± 0.002	28.992 ± 0.002	46
CH <sub>3</sub>	35.8 ± 0.1	35.0 ± 0.1	46
COCl	-5.6 ± 0.7	-5.2 ± 0.6	47
CH <sub>2</sub> =C=O	-10.6 ± 0.4	-11.4 ± 0.4	48
HCl	-22.02 ± 0.02	-22.06 ± 0.02	46
CH <sub>3</sub> Cl	-17.673 ± 0.01	-19.57 ± 0.01	46
CO	-27.201 ± 0.04	-26.42 ± 0.04	46, 49
CH <sub>3</sub> CO <sup>+</sup>	156.5 ± 2.0	157.0 ± 0.4	50
Cl <sup>-</sup>	-54.751 ± 0.05	-55.85 ± 0.05	46
CH <sub>3</sub> CH <sub>2</sub> COCl	-59.8 ± 1.4	-63.0 ± 1.0	18, 51
CH <sub>3</sub> CH <sub>2</sub> CO	-5.3 ± 0.5	-7.7 ± 0.4	52
CH <sub>3</sub> CH <sub>2</sub>	31.5 ± 0.5	28.9 ± 0.4	53, 54
CH <sub>3</sub> CH=C=O	-20.4 ± 3.5	-22.7 ± 1.2	55, 56
CH <sub>3</sub> CH <sub>2</sub> Cl	-23.33 ± 0.19	-26.81 ± 0.19	57
CH <sub>2</sub> =CH <sub>2</sub>	14.56 ± 0.12	12.52 ± 0.12	46
CH <sub>3</sub> CH <sub>2</sub> CO <sup>+</sup>	141.5 ± 3.3	141.3 ± 0.3	58
CH <sub>3</sub> CHO	-37.2 ± 0.1	-39.7 ± 0.1	19, 20
H	51.634 ± 0.001	52.103 ± 0.001	46
CH <sub>3</sub> COCH <sub>3</sub>	-48.0 ± 0.2	-51.9 ± 0.2	19, 20
CH <sub>3</sub> COOH	-100.0 ± 0.4	-103.3 ± 0.4	19, 20
OH	9.35 ± 0.05	9.40 ± 0.05	46
CH <sub>3</sub> CH <sub>2</sub> CHO	-42.8 ± 1.6	-45.09 ± 0.18	59, 60
CH <sub>3</sub> CH <sub>2</sub> COCH <sub>3</sub>	-50.0 ± 2.4	-57.1 ± 0.2	20, 61
CH <sub>3</sub> CH <sub>2</sub> COCH <sub>2</sub> CH <sub>3</sub>	-53.3 ± 3.5	-61.6 ± 0.2	20, 62
CH <sub>3</sub> CH <sub>3</sub>	-16.34 ± 0.10	-20.08 ± 0.10	46

with the radical pair, this would be followed by caging and recombination producing a “hot” ground-state molecule (20).



The “hot” ground-state system will undergo thermal decomposition as with the radical pair (15, 16). We believe the ion–ion process is unlikely based on thermochemical grounds (vide infra); formation of the ion pair requires more energy (148.5 ± 1.0 kcal mol<sup>-1</sup>) than is available from the excitation.

In the radical–radical mechanism, the role of the Ar matrix is passive; its only function is to trap the radical pair, allowing the subsequent radical–radical chemistry to occur. In the other two cases, the Ar matrix has changed the nature of the electronic surfaces accessed by the photoexcitation and altered the reaction outcome by either inhibiting the gas-phase channel or making a new channel accessible.

**Thermochemistry.** The thermochemistry of acetyl chloride dissociation in the gas phase can be determined from the experimental heats of formation for the various species involved (Table 4). Using these values, we determine the bond energy of the C–Cl bond in CH<sub>3</sub>COCl to be  $DH_{298}(\text{CH}_3\text{CO}-\text{Cl}) = 84.6 \pm 0.4 \text{ kcal mol}^{-1}$ ; this value has been previously<sup>16</sup> reported as  $83.2 \pm 0.4 \text{ kcal mol}^{-1}$ . The C–C bond energy is computed to be  $DH_{298}(\text{CH}_3-\text{COCl}) = 87.8 \pm 0.6 \text{ kcal mol}^{-1}$ . Thus the initial CH<sub>3</sub>COCl fragmentation in the gas phase occurs at the weaker of the two α-bonds, consistent with the findings of Arunan.<sup>17</sup> Reaction enthalpies for various reaction channels of acetyl chloride are collected in Table 5. There may be enough internal energy remaining in the CH<sub>3</sub>CO to exceed the threshold,  $DH_{298}(\text{CH}_3-\text{CO}) = 10.2 \pm 0.3 \text{ kcal mol}^{-1}$ , for further dissociation.

The thermochemistry of CH<sub>3</sub>CH<sub>2</sub>COCl dissociation has not been experimentally determined, but we can reasonably estimate it. The heat of formation of propionyl chloride is estimated to be  $\Delta_f H_{298}(\text{CH}_3\text{CH}_2\text{COCl}) = -63 \text{ kcal mol}^{-1}$  by Benson’s method<sup>18</sup> of group equivalents. As a check of the group

TABLE 5: Heats of Reactions for Acid Chloride Dissociation

reaction	$\Delta_{\text{rxn}} H_0/\text{kcal mol}^{-1}$	$\Delta_{\text{rxn}} H_{298}/\text{kcal mol}^{-1}$
CH <sub>3</sub> COCl → CH <sub>3</sub> CO + Cl	83.6 ± 0.4	84.6 ± 0.4
CH <sub>3</sub> COCl → CH <sub>3</sub> + COCl	86.1 ± 0.7	87.8 ± 0.6
CH <sub>3</sub> COCl → CH <sub>2</sub> CO + HCl	23.3 ± 0.4	24.5 ± 0.4
CH <sub>3</sub> COCl → CH <sub>3</sub> Cl + CO	11.0 ± 0.2	12.0 ± 0.2
CH <sub>3</sub> COCl → CH <sub>3</sub> + CO + Cl	93.1 ± 0.2	95.6 ± 0.2
CH <sub>3</sub> CO → CH <sub>3</sub> + CO	9.5 ± 0.3	11.0 ± 0.3
COCl → Cl + CO	7.0 ± 0.7	7.8 ± 0.6
CH <sub>3</sub> CO + Cl → CH <sub>2</sub> CO + HCl	-60.3 ± 0.5	-60.1 ± 0.5
CH <sub>3</sub> CO + Cl → CH <sub>3</sub> Cl + CO	-72.6 ± 0.3	-72.6 ± 0.3
CH <sub>3</sub> + COCl → CH <sub>2</sub> CO + HCl	-62.8 ± 0.8	-63.3 ± 0.7
CH <sub>3</sub> + COCl → CH <sub>3</sub> Cl + CO	-75.1 ± 0.7	-75.8 ± 0.6
CH <sub>3</sub> + Cl → CH <sub>3</sub> Cl	-82.1 ± 0.1	-83.6 ± 0.1
CH <sub>3</sub> COCl → CH <sub>3</sub> CO <sup>+</sup> + Cl <sup>-</sup>	157.6 ± 2.1	159.2 ± 0.4
CH <sub>3</sub> CH <sub>2</sub> COCl → CH <sub>3</sub> CH <sub>2</sub> CO + Cl	83.1 ± 1.5	84.3 ± 1.1
CH <sub>3</sub> CH <sub>2</sub> COCl → CH <sub>3</sub> CH <sub>2</sub> + COCl	85.7 ± 1.7	86.7 ± 1.2
CH <sub>3</sub> CH <sub>2</sub> COCl → CH <sub>3</sub> CH <sub>2</sub> + CO + Cl	92.7 ± 1.5	94.5 ± 1.1
CH <sub>3</sub> CH <sub>2</sub> COCl → CH <sub>3</sub> + CH <sub>2</sub> CO + Cl	113.6 ± 1.5	115.6 ± 1.1
CH <sub>3</sub> CH <sub>2</sub> COCl → CH <sub>3</sub> CHCO + HCl	17.5 ± 3.8	18.2 ± 1.6
CH <sub>3</sub> CH <sub>2</sub> COCl → CH <sub>2</sub> CH <sub>2</sub> + CO + HCl	25.2 ± 1.4	27.0 ± 1.0
CH <sub>3</sub> CH <sub>2</sub> COCl → CH <sub>3</sub> CH <sub>2</sub> Cl + CO	9.3 ± 1.5	9.8 ± 1.0
CH <sub>3</sub> CH <sub>2</sub> COCl → CH <sub>3</sub> COCl + CH <sub>2</sub> CO	31.6 ± 1.5	32.0 ± 1.1
CH <sub>3</sub> CH <sub>2</sub> CO → CH <sub>3</sub> CH <sub>2</sub> + CO	9.6 ± 0.7	10.2 ± 0.6
CH <sub>3</sub> CH <sub>2</sub> CO + Cl → CH <sub>3</sub> CHCO + HCl	-65.7 ± 3.6	-66.0 ± 1.3
CH <sub>3</sub> CH <sub>2</sub> CO + Cl → CH <sub>2</sub> CH <sub>2</sub> + CO + HCl	-57.9 ± 0.6	-57.2 ± 0.5
CH <sub>3</sub> CH <sub>2</sub> CO + Cl → CH <sub>3</sub> CH <sub>2</sub> Cl + CO	-73.8 ± 0.6	-74.5 ± 0.5
CH <sub>2</sub> CH <sub>2</sub> + HCl → CH <sub>3</sub> CH <sub>2</sub> Cl	-15.9 ± 0.2	-17.3 ± 0.2
CH <sub>3</sub> CH <sub>2</sub> COCl → CH <sub>3</sub> CH <sub>2</sub> CO <sup>+</sup> + Cl <sup>-</sup>	146.5 ± 3.6	148.5 ± 1.0

equivalents method, we calculate  $\Delta_f H_{298}(\text{CH}_3\text{COCl}) = -58.0 \text{ kcal mol}^{-1}$ , which is identical to the published experimental value.<sup>19,20</sup> Using the values from Table 4, we compute  $DH_{298}(\text{CH}_3\text{CH}_2\text{CO}-\text{Cl})$  as  $84.3 \pm 1.1 \text{ kcal mol}^{-1}$  and  $DH_{298}(\text{CH}_3\text{CH}_2-\text{COCl})$  as  $86.7 \pm 1.2 \text{ kcal mol}^{-1}$ . Other reaction energies for propionyl chloride dissociation are given in Table 5. A 266-nm photon (107.5 kcal mol<sup>-1</sup>) will have enough energy to break the C–Cl bond in CH<sub>3</sub>CH<sub>2</sub>COCl and should deposit enough extra energy in the fragments to drive subsequent reaction(s).

Fragmentation into an ion pair, RCO<sup>+</sup> + Cl<sup>-</sup>, requires 159.2 ± 0.4 kcal mol<sup>-1</sup> for CH<sub>3</sub>COCl and 148.5 ± 1.0 kcal mol<sup>-1</sup> for CH<sub>3</sub>CH<sub>2</sub>COCl at 298 K (Table 5). None of the wavelengths, 266 nm (107.5 kcal mol<sup>-1</sup>), 254 nm (112.6 kcal mol<sup>-1</sup>), or 248 nm (115.3 kcal mol<sup>-1</sup>), used in these experiments provide that much energy. For ion pairs to be formed, the stabilization by the Ar matrix will be decisive. Even though the polarizability<sup>21</sup> of Ar (1.6 Å<sup>3</sup>) is about 1/4 that of CH<sub>3</sub>CN (4.4 Å<sup>3</sup>), it seems that the formation of a carbonyl ion and chloride ion, [RCO<sup>+</sup>, Cl<sup>-</sup>], is unlikely on energetic grounds. Thus we believe that fragmentation into an ion pair is not a likely mechanism for the decomposition of acid chlorides in the argon matrix.

**“Kinetics” of Decomposition.** Spectra collected during the irradiation track the progress of the photodecomposition. The change in the integrated area for any IR feature as the decomposition proceeds can be used to calculate a growth or decay profile for that feature. The area of an absorption feature<sup>22</sup> can be related to the number of molecules of a particular species,  $n/\text{cm}^{-3}$ , by the integrated absorption cross section,  $A/\text{km mol}^{-1}$ . Our FTIR spectrometer records the optical density,  $\text{OD} \equiv \log(I_0/I)$ , and we use the optical path length through the matrix,  $z/\text{cm}^{-1}$ .

$$\int_{\text{IRband}} \text{OD}(\nu) d\nu = n \frac{Az}{\ln(10)} \quad (21)$$

The path length,  $z$ , is fixed when the matrix is deposited and does not change during the experiment, and the cross section is

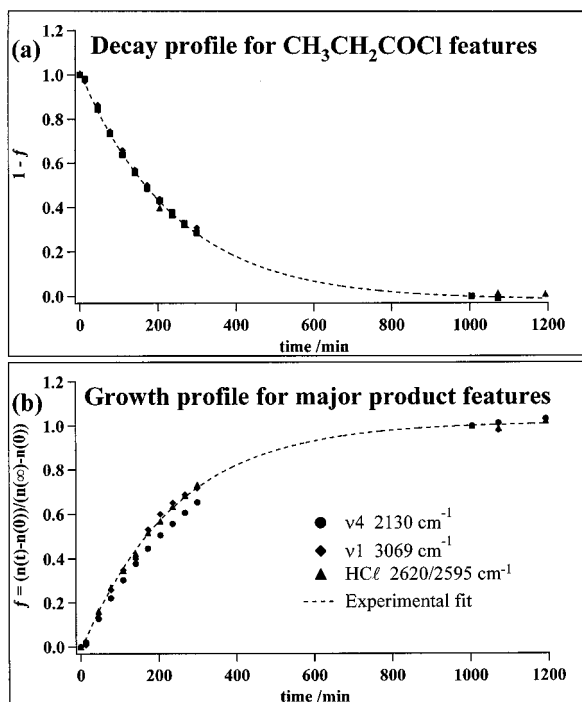


**Figure 7.** Kinetics curves for the photodissociation of propionyl chloride in an Ar matrix during irradiation at 254 nm. The decay of several precursor features is tracked in (a) while the growth of several major product features is tracked in (b). The decay data for the C=O stretching mode of  $\text{CH}_3\text{CH}_2\text{COCl}$  at  $1803\text{ cm}^{-1}$  was fit to an exponential curve, and that fit was reversed and plotted in (b).

a constant of the molecule. The peak area at any time during the irradiation is thus directly proportional to the number of molecules at that time. The normalized fraction of molecules present at any time,  $f(t)$ , is found by taking the area, subtracting the area over the same range in the initial spectrum, and normalizing that difference by the difference between the areas in the final ( $t \rightarrow \infty$ ) and initial ( $t = 0$ ) spectra.

$$f(t) = \frac{A(t) - A(0)}{A(\infty) - A(0)} = \frac{n(t) - n(0)}{n(\infty) - n(0)} \quad (22)$$

Expression 22 gives a fraction between 0 and 1 that indicates the extent of the decomposition of the precursor or the growth of the product at each point in time from the initial spectrum to the final spectrum (chosen at a time when most of the precursor is dissociated). All features belonging to the same species will have the same profile. Features due to product molecules from the same reaction channel should grow in at the same rate; if there is only one active decomposition channel, the precursor peaks should decay at that same rate. Figure 7 shows the curves resulting from this analysis for some of the stronger precursor and product features during irradiation at 254 nm. A first-order decay fit for the experimental data of the strongest precursor peak is also shown. The main features assigned to the precursor and those of the products all display the same first-order behavior, suggesting that only one reaction channel is active for propionyl chloride photodecomposition in an Ar matrix at 254 nm. It is clear from the photoproducts that this is an  $\alpha$ -abstraction or elimination channel (13, 15, 18).

**Orientation of Products.** Polarization studies were conducted to determine the relative orientation of the product methyl ketene and HCl molecules in the Ar matrix. Linearly polarized UV 266-nm light was used to irradiate the sample; the axis of polarization defines a unique axis,  $Z$ , in the lab frame. IR

**TABLE 6: Dichroic Ratio and Orientation Factors**

	mode	$I(0^\circ)/I(90^\circ)$	$K$	$I(180^\circ)/I(270^\circ)$	$K$	
a'	$\nu_1$	1.20	0.375	1.24	0.382	
	$\nu_2$	1.10	0.354	1.07	0.349	
	$\nu_3$	1.10	0.355	1.13	0.360	
	$\nu_4$	1.12	0.360	1.13	0.360	
	$\nu_5$	1.10	0.356	1.34	0.403	
	$\nu_9$	1.08	0.350	0.911	0.313	
	$\nu_{10}$	1.08	0.350	1.10	0.355	
	$\nu_{11}$	1.00	0.333	0.979	0.328	
	a''	$\nu_{14}$	0.738	0.270	0.756	0.275
		$\nu_{16}$	0.825	0.292	0.821	0.291
		$\nu_{17}$	0.957	0.324	0.827	0.293
HCl		0.766	0.277	0.766	0.277	

absorption spectra of the matrix were recorded using IR light polarized at various angles,  $\theta$ , with respect to the polarization axis of the initial irradiation. When IR light polarized along the  $Z$ -axis is passed through the sample ( $\theta = 0^\circ$ ), the integrated intensity for a given mode will be proportional to the projection of the transition dipole on the  $Z$ -axis.<sup>23,24</sup>

$$I(0^\circ) = A \langle \cos^2(\alpha_i) \rangle \quad (23)$$

$A$  is related to the absorption cross section of the mode,  $\alpha_i$  is the angle between the transition moment for the  $i$ th molecule and the  $Z$ -axis, and the pointed brackets indicate averaging over all molecules in the sample. The integrated intensity for IR light polarized at  $\theta = 90^\circ$  will be given similarly.

$$I(90^\circ) = 1/2 A [1 - \langle \cos^2(\alpha_i) \rangle] \quad (24)$$

By taking the ratio of these two equations, we can solve for the average of the square of the cosines, a value defined as the orientation factor,  $K$ .

$$K = \langle \cos^2(\alpha_i) \rangle = \frac{I(0^\circ)/I(90^\circ)}{[2 + I(0^\circ)/I(90^\circ)]} \quad (25)$$

The ratio  $I(0^\circ)/I(90^\circ)$  is called the dichroic ratio,  $d$ . For an isotropically distributed sample,  $K = 1/3$ ; in the limit where all transition moments are oriented along the  $Z$ -axis,  $K = 1$ , and in the other limit,  $K = 0$ . In a molecule with three or more symmetry axes, the transition moment for any absorption will be directed along one of three mutually perpendicular axes in the molecular frame, and there will be three unique values for the dichroic ratio in an anisotropic sample. For an anisotropic sample of a molecule with  $C_s$  symmetry, such as methyl ketene, all of the modes whose dipole transition moment is perpendicular to the plane (a'' modes) will have the same dichroic ratio. (Since the dipoles will all be directed along the same axis in the molecular frame, they will have the same average angle to the  $Z$ -axis over the ensemble.) Table 6 gives the dichroic ratio and orientation factors for some of the modes in methyl ketene, as well as for the HCl stretch. The dichroic ratio was calculated using both  $I(0^\circ)/I(90^\circ)$  and  $I(180^\circ)/I(270^\circ)$ ; the two values should be the same for a given mode. The HCl stretch has the same dichroic ratio as all of the a'' modes, consistent with a  $[\text{CH}_3\text{CH}=\text{C}=\text{O}, \text{HCl}]$  complex in which the HCl is situated perpendicular to the plane of the methyl ketene.

The normalized integrated peak area for an IR feature plotted as a function of the IR polarization angle can also tell us about the orientation of the dipole moment for that absorption relative to the initial polarization axis. Figure 8 shows these curves for several of the stronger product absorptions, including the methyl ketene  $\nu_4$  C=C=O stretching mode (a' symmetry) at  $2130\text{ cm}^{-1}$

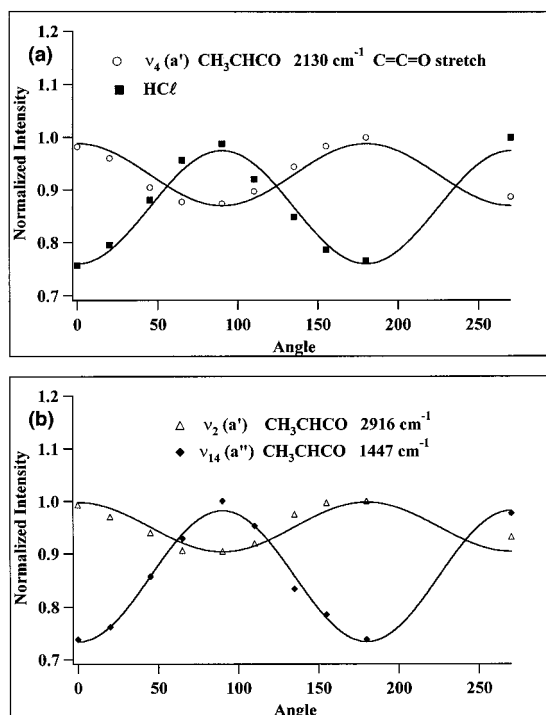


**Figure 8.** Angular dependence for  $\text{CH}_3\text{CHCO}$  and  $\text{HCl}$  modes following irradiation with linear polarized UV light. An angle of  $0^\circ$  corresponds to the IR polarizer set along the axis of the UV laser polarization.

and the  $\text{HCl}$  stretch around  $2600\text{ cm}^{-1}$ . These data is fitted with the functional form

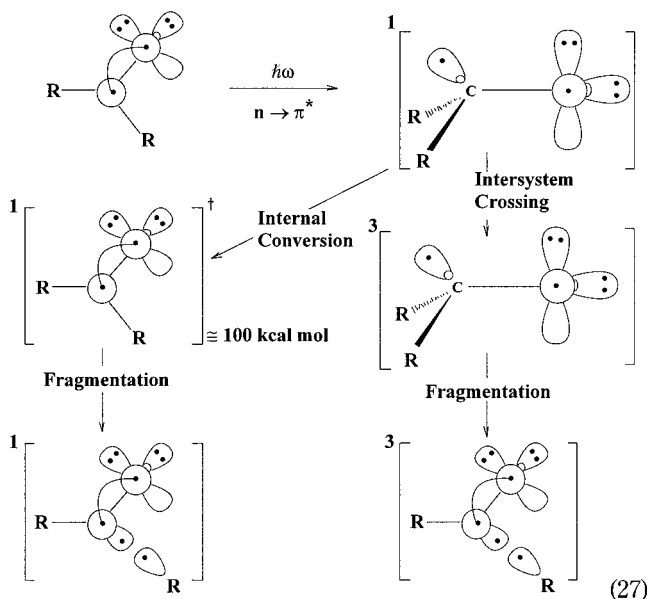
$$I(\theta) = A[\cos^2(\theta + \phi) + \cos^2(\theta - \phi)] \quad (26)$$

where  $A$  gives information about the degree of orientation and  $\phi$  gives the average angle of the transition dipole about the polarization axis of the UV irradiation. It is found that all methyl ketene IR modes assigned with  $a'$  symmetry have a similar angle dependence as the  $\nu_4$  mode, while  $\text{HCl}$  behaves like the  $a''$  methyl ketene modes. This again suggests that the  $\text{HCl}$  molecule is oriented perpendicular to the plane of the methyl ketene.

It is reasonable to expect that  $\text{HCl}$  formed in an abstraction reaction would be aligned perpendicular to the  $\text{C}=\text{C}=\text{O}$  structure; following the abstraction, the hydrogen atom could swing toward the ketene to hydrogen bond with the  $\text{C}=\text{C}=\text{O}$   $\pi$ -electrons. The result would be a complex with the hydrogen in the  $\text{HCl}$  situated between the chlorine atom and the  $\text{C}=\text{C}=\text{O}$  of the methyl ketene. However, in this case we would not expect the  $\text{HCl}$  to be specifically oriented with respect to the plane of the methyl ketene but rather distributed around the  $\text{C}=\text{C}=\text{O}$  axis. That the  $\text{HCl}$  is oriented preferentially perpendicular to the plane of the methyl ketene suggests that the reaction proceeds via an elimination pathway (15, 18) as opposed to hydrogen abstraction (13), and that no free chlorine atom is generated during the photolysis.

**The Mechanism of Acid Chloride Photolysis.** The photochemical cleavage of the  $\alpha$ -bond in ketones and aldehydes is titled a Norrish type I mechanism. The accepted gas-phase mechanism<sup>25–27</sup> for this complicated fragmentation is summarized in (27) (Scheme 1). Optical excitation of the carbonyl group<sup>28</sup> produces an  $\tilde{A}^1(n\pi^*)$ ,  $^1A''$  state. In a  $C_{2v}$  molecule such as  $\text{CH}_2\text{O}$  or  $(\text{CH}_3)_2\text{CO}$ , this is a dipole-forbidden  $\tilde{A}^1A_2 \leftarrow \tilde{X}^1A_1$  transition, which occurs<sup>29</sup> between 333 and 285 nm ( $86$ – $100\text{ kcal mol}^{-1}$ ). The  $C_s$  molecules such as  $\text{CH}_3\text{CHO}$  and

### SCHEME 1



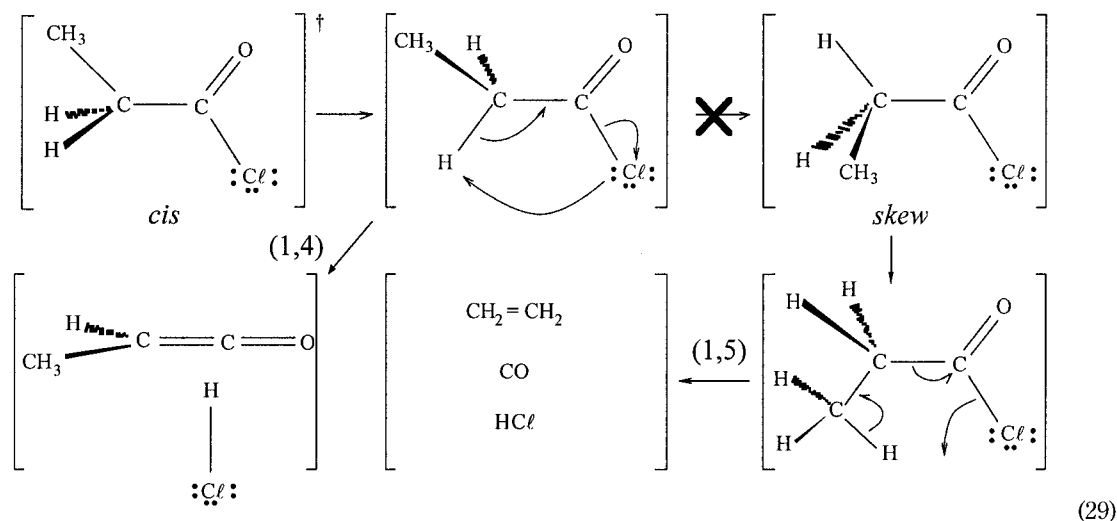
$\text{CH}_3\text{CH}_2\text{CHO}$  possess weak, featureless absorptions peaking at roughly 285 nm. Internal conversion<sup>28</sup> from the  $\tilde{A}^1(n\pi^*)$ ,  $^1A''$  state to  $\tilde{X}^1A'$  produces an excited (“hot”) ground state, which spontaneously undergoes  $\alpha$ -bond cleavage. Alternatively, intersystem crossing leads to the  $\tilde{a}^3(n\pi^*)$ ,  $^3A''$  state, which has a barrier to fragmentation that (qualitatively) arises from the crossing of the  $^3(n\pi^*)$  and  $^3(\sigma\sigma^*)$  states. If the system surmounts the barrier, dissociation occurs via the  $\tilde{a}^3(n\pi^*)$ ,  $^3A''$  state. The result of a Norrish type I cleavage is a radical pair.

In contrast to the “conventional” Norrish type I cleavage, gas-phase photofragmentation in acid chlorides has recently been shown to be a rapid, excited-state process.<sup>4,7,8</sup> Excitation to the lowest electronic state of  $\text{CH}_3\text{COCl}$  occurs at about 240 nm ( $119\text{ kcal mol}^{-1}$ ). The photoelectron spectrum<sup>30</sup> of  $\text{CH}_3\text{COCl}$  provides the ionization potential of  $\text{IP}(\text{CH}_3\text{COCl}) = 11.03 \pm 0.02\text{ eV}$ , and the ground state of the  $\text{CH}_3\text{COCl}^+$  ion is assigned as  $\tilde{X}^2A'$ . The ionization spectrum of  $\text{CH}_3\text{COCl}$  is quite similar to that of  $\text{CH}_2\text{O}$  and  $\text{CH}_3\text{CHO}$ , and the vibronic structure clearly identifies the frontier orbital of  $\text{CH}_3\text{COCl}$  as  $16a'$ , a nonbonding orbital centered on both O and Cl. For these reasons, one is confident that the 242-nm band seen in  $\text{CH}_3\text{COCl}$  and also in  $\text{CH}_3\text{CH}_2\text{COCl}$  in Figure 5 belongs to a  $^1(\pi^* \leftarrow n)$  transition. The transition dipole moment for this absorption is oriented<sup>4</sup> consistent with this assignment.

When  $\text{CH}_3\text{COCl}$  is excited<sup>7,8</sup> in a supersonic molecular beam with an excimer laser at 248 nm and the photofragments collected, the initial event is described by (1), fragmentation to the acetyl radical and atomic chlorine. The photofragments are  $\text{Cl}$  and  $\text{CH}_3\text{CO}$ , and the angular distribution of the  $\text{Cl}$  species is strongly peaked with an anisotropy factor of  $\beta = 1.0 \pm 0.2$ . Such a distribution of photofragments clearly shows that the  $\text{Cl}$  atom is ejected in  $<1\text{ ps}$ , and it may even occur within 200 fs.<sup>4</sup> Consequently the photodissociation of  $\text{CH}_3\text{COCl}$  is not a conventional Norrish type I process (27) but proceeds<sup>7,8</sup> via a rapid curve crossing from a  $^1(\pi^* \leftarrow n)$  state to a  $^1(\sigma^* \leftarrow n\pi)$  curve. This cleaves only the  $\text{C}-\text{Cl}$  in the primary dissociation, producing a “hot” acetyl radical; the  $\text{C}-\text{C}$  bond is never fractured in the primary dissociation. Studies of the photofragmentation of acetyl chloride at 236 nm ( $121\text{ kcal mol}^{-1}$ ) have shown that the  $\text{CH}_3\text{CO}$  is formed with a mean  $19\text{ kcal mol}^{-1}$  internal energy following photodissociation.<sup>5,6</sup> The barrier to dissociation of the acetyl radical into  $\text{CH}_3$  and  $\text{CO}$



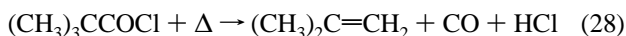
## SCHEME 2



has been measured<sup>31–33</sup> at around 17 kcal mol<sup>-1</sup>, so a significant fraction of these CH<sub>3</sub>CO radicals will have enough energy for further fragmentation to produce CO and CH<sub>3</sub> radicals.

Experiments that probed for a free chlorine atom in the matrix showed<sup>34</sup> that no atomic chlorine is produced during the photolysis of acetyl chloride at 266 nm in the condensed phase. Thus the mechanism for CH<sub>3</sub>COCl dissociation in the condensed phase is known to be an elimination mechanism, II, and not a radical pair process, I. We believe propionyl chloride, and all alkyl acid chlorides, will photodecompose this way in the condensed phase; CH<sub>3</sub>CH<sub>2</sub>COCl decomposes through the direct elimination of HCl (18).

Since atomic chlorine is not produced in condensed-phase acid chloride photodecomposition, the gas-phase curve crossing from a <sup>1</sup>(π\* ← n) state to a <sup>1</sup>(σ\* ← np) state must be altered by the presence of the surrounding matrix. With this channel inhibited, the system relaxes through internal conversion on a singlet surface to form a “hot” ground-state molecule.<sup>1</sup> The “hot” acid chloride ground state, [CH<sub>3</sub>CH<sub>2</sub>COCl]<sup>†</sup>, undergoes an electrocyclic elimination<sup>35,36</sup> to produce CH<sub>3</sub>CHCO and HCl. This process has been observed in acid chlorides. CH<sub>3</sub>COCl is known to thermally decompose at 820 K in the injection port of a photoionization spectrometer:<sup>37</sup> CH<sub>3</sub>COCl + Δ → CH<sub>2</sub>=CO + HCl. The barrier for HCl elimination in acetyl chloride has been computed<sup>38</sup> by ab initio electronic structure calculations to be 48 kcal mol<sup>-1</sup>, which is lower than the activation energy reported<sup>39</sup> for thermal elimination of HCl from trimethyl acetyl chloride, (CH<sub>3</sub>)<sub>3</sub>CCOCl, 55.2 kcal mol<sup>-1</sup>.



The latter is a (1, 5)-elimination (β-elimination) process, while the former is a (1, 4)-elimination (α-elimination). (For comparison, a barrier of 58.430 ± 1.500 kcal mol<sup>-1</sup> has been reported<sup>40</sup> for HCl elimination from CH<sub>3</sub>CH<sub>2</sub>Cl, and a barrier of 53.97 ± 1.19 kcal mol<sup>-1</sup> has been reported<sup>41</sup> for HCl elimination from CD<sub>2</sub>HCD<sub>2</sub>Cl.) In propionyl chloride, the α-elimination channel requires Δ<sub>rxn</sub>H<sub>298</sub> = 18.2 ± 1.6 kcal mol<sup>-1</sup> while β-elimination requires Δ<sub>rxn</sub>H<sub>298</sub> = 27.0 ± 1.0 kcal mol<sup>-1</sup>, so α-elimination is energetically preferred. However, given the photon energies used (>100 kcal mol<sup>-1</sup>), one might expect enough energy in the system to overcome the barrier for either elimination in the thermal ground state.

Why are there no products from the β-elimination channel (19) for propionyl chloride? This is likely a second matrix effect. In the gas-phase propionyl fluoride, CH<sub>3</sub>CH<sub>2</sub>COF, exists in two rotational conformers, *cis* and *skew*;<sup>9,42</sup> the barrier for rotation from the more stable *cis* to the *skew* conformer is 2.400 ± 0.060 kcal mol<sup>-1</sup>. The analogous acid chloride, CH<sub>3</sub>CH<sub>2</sub>COCl is also thought to have these two conformers in the gas phase.<sup>9</sup> In the *cis* conformer, the dihedral angle for the CCCO skeleton is 0°, while in the *skew* structure it is 120°. In the condensed phase only the more stable *cis* conformer is observed.<sup>9</sup> With rotation about the C–C bond restricted by the matrix, we see photodecomposition products from a (1, 4)-elimination, which is more likely from the *cis* conformation. Thus the condensed-phase decomposition for propionyl chloride may be pictured as in Scheme 2.

The [CH<sub>3</sub>CH=C=O, HCl] pair from the electrocyclic elimination in the matrix forms a complex that is roughly T-shaped. Note that in order for a (1, 5)-elimination to occur in the matrix, the methyl group must rotate 180° around the C–C bond from the *cis* conformer. Given the constraints in the matrix, this is not likely.

## 5. Conclusions

We have found that propionyl chloride, CH<sub>3</sub>CH<sub>2</sub>COCl, photodissociates to form exclusively methyl ketene, CH<sub>3</sub>CH=CO, and HCl in an Ar matrix following excitation of the <sup>1</sup>(π\* ← n) transition around 242 nm. We believe the decomposition occurs on the ground state following internal conversion on a singlet surface from the initially excited state. This decomposition process is completely different than the gas-phase process, which involves a rapid cleavage of the C–Cl bond following excitation of the same transition. This difference is also seen between gas- and condensed-phase acetyl chloride and will likely be the case for all alkyl acid chlorides. The major effect of the matrix is to shift the electronic states involved in the rapid curve crossing from a <sup>1</sup>(π\* ← n) state to a <sup>1</sup>(σ\* ← np) state, which occurs in the gas-phase dissociation. In the condensed phase, the molecule instead proceeds along a conventional Norrish type I pathway (27), with internal conversion on a singlet surface to the ground state, followed by thermal ground-state chemistry. We are currently investigating the photodecomposition of (CH<sub>3</sub>)<sub>3</sub>CCOCl and C<sub>6</sub>H<sub>5</sub>COCl to determine the behavior of acid chlorides in the absence of α-hydrogen atoms.

**Acknowledgment.** The authors were supported by the Division of Chemical Sciences of the Office of Basic Energy Sciences, U.S. Department of Energy. Pacific Northwest National Laboratory is operated for the U.S. Department of Energy by Battelle under Contract DE-AC06-76RLO 1830. This collaboration has been funded by Associated Western Universities Incorporated. G.B.E. and P.R.W. are grateful to the National Science Foundation (CHE-9215164) for support. M.R.N. and J.G.R. were supported by internal funds at the National Renewable Energy Laboratory (FIRST Program).

## References and Notes

- (1) Rowland, B.; Hess, W. P. *J. Phys. Chem. A* **1997**, *101*, 8049.
- (2) Rowland, B.; Hess, W. P. *Chem. Phys. Lett.* **1996**, *263*, 574.
- (3) Kogure, N.; Ono, T.; Watari, F. *J. Mol. Struct.* **1993**, *296*, 1.
- (4) Shibata, T.; Suzuki, T. *Chem. Phys. Lett.* **1996**, *262*, 115.
- (5) Deshmukh, S.; Hess, W. P. *J. Chem. Phys.* **1994**, *100*, 6429.
- (6) Deshmukh, S.; Hess, W. P. *J. Phys. Chem.* **1994**, *98*, 12535.
- (7) Person, M. D.; Kash, P. W.; Butler, L. J. *J. Chem. Phys.* **1992**, *97*, 355.
- (8) Person, M. D.; Kash, P. W.; Butler, L. J. *J. Phys. Chem.* **1992**, *96*, 2021.
- (9) Frankiss, S. G.; Kynaston, W. *Spectrochim. Acta* **1975**, *31A*, 661.
- (10) Kappe, C. O.; Wong, M. W.; Wentrup, C. J. *Org. Chem.* **1995**, *60*, 1686.
- (11) Harrison, J. A.; Frei, H. *J. Phys. Chem.* **1994**, *98*, 12142.
- (12) Frisch, M. J.; Trucks, G. W.; Schlegel, H. B.; Gill, P. M. W.; Johnson, B. G.; Robb, M. A.; Cheeseman, J. R.; Keith, T.; Petersson, G. A.; Montgomery, J. A.; Raghavachari, K.; Al-Laham, M. A.; Zakrzewski, V. G.; Ortiz, J. V.; Foresman, J. B.; Cioslowski, J.; Stefanov, B. B.; Nanayakkara, A.; Challacombe, M.; Peng, C. Y.; Ayala, P. Y.; Chen, W.; Wong, M. W.; Andres, J. L.; Replogle, E. S.; Gomperts, R.; Martin, R. L.; Fox, D. J.; Binkley, J. S.; Defrees, D. J.; Baker, J.; Stewart, J. P.; Head-Gordon, M.; Gonzalez, C.; Pople, J. A. *Gaussian 94*, Revision C.2; Gaussian, Inc.: Pittsburgh, PA, 1996.
- (13) Cowieson, D. R.; Barnes, A. J.; Orville-Thomas, W. J. *J. Raman Spectrosc.* **1981**, *10*, 224.
- (14) Shimanouchi, T. *Tables of Molecular Vibrational Frequencies*; National Bureau of Standards: Washington, DC, 1972; Vol. I.
- (15) Hongzhi, L.; Qiang, L.; Wentao, M.; Qihe, Z.; Fanao, K. *J. Chem. Phys.* **1997**, *106*, 5943.
- (16) Devore, J. A.; O'Neal, H. E. *J. Phys. Chem.* **1969**, *73*, 2644. These workers report  $DH_{298}(\text{CH}_3\text{CH}_2\text{CO}-\text{Cl}) = 83.2 \pm 0.4 \text{ kcal mol}^{-1}$ .
- (17) Arunan, E. *J. Phys. Chem. A* **1997**, *101*, 4838.
- (18) Benson, S. W. *Thermochemical Kinetics*, 2nd ed.; John Wiley & Sons: New York, 1976.
- (19) Wiberg, K. B.; Hadad, C. M.; Rablen, P. R.; Cioslowski, J. *J. Am. Chem. Soc.* **1992**, *114*, 8644.
- (20) Pedley, J. B.; Naylor, R. D.; Kirby, S. P. *Thermochemical Data of Organic Compounds*, 2nd ed.; Chapman and Hall Ltd: London, 1986.
- (21) Miller, T. M. Atomic and Molecular Polarizabilities. In *Handbook of Chemistry and Physics*, 66th ed.; Weast, R. C., Ed.; CRC Press: Boca Raton, FL, 1985; p E-65.
- (22) Pugh, L. A.; Narahari Rao, K. Intensities From Infrared Spectra. In *Molecular Spectroscopy: Modern Research*; Rao, K. N., Ed.; Academic Press: New York, 1976; Vol. II, p 165.
- (23) Michl, J.; Thulstrup, E. W. *Spectroscopy with Polarized Light. Solute Alignment by Photoselection, in Liquid Crystals, Polymers, and Membranes*; VCH: New York, 1986.
- (24) Radziszewski, J. G.; Downing, J. W.; Gudipati, M. S.; Balaji, V.; Thulstrup, E. W.; Michl, J. *J. Am. Chem. Soc.* **1996**, *118*, 10275.
- (25) Dauben, W. G.; Salem, L.; Turro, N. J. *Acc. Chem. Res.* **1975**, *8*, 41.
- (26) Turro, N. J. *Modern Molecular Photochemistry*; Benjamin/Cummings Publishing Co.: Menlo Park, CA, 1978.
- (27) Kopecký, J. *Organic Photochemistry: A Visual Approach*; VCH Publishers: New York, 1992.
- (28) Michl, J.; Bonácić-Koutecký, V. *Electronic Aspects of Organic Photochemistry*; John Wiley & Sons: New York, 1990.
- (29) Robin, M. B. *Higher Excited States of Polyatomic Molecules*; Academic Press: New York, 1975; Vol. II.
- (30) Kimura, K.; Katsumata, S.; Achiba, Y.; Yamazaki, T.; Iwata, S. *Handbook of He I Photoelectron Spectra of Fundamental Organic Molecules*; Halsted Press: New York, 1980.
- (31) North, S. W.; Blank, D. A.; Gezelter, J. D.; Longfellow, C. A.; Lee, Y. T. *J. Chem. Phys.* **1995**, *102*, 4447.
- (32) North, S.; Blank, D. A.; Lee, Y. T. *Chem. Phys. Lett.* **1994**, *224*, 38.

- (33) Watkins, K. W.; Word, W. W. *Int. J. Chem. Kinet.* **1974**, *7*, 885.
- (34) Rowland, B.; Hess, W. P. *J. Phys. Chem. A* **1997**, *101*, 8049. Rowland and Hess photolyzed  $\text{Cl}_2$  and acetyl chloride in a propane matrix and searched for the products of reactions between the  $\text{Cl}$  and  $\text{CH}_3\text{CH}_2\text{CH}_3$ . When  $\text{Cl}_2$  was photolyzed in a propane matrix, propene, 2-chloropropane, and 1-chloropropane were among the products observed. When acetyl chloride was irradiated at 193 nm, these same products were observed. Irradiation at 193 nm excites  $\text{CH}_3\text{COCl}$  directly to a dissociative state, so chlorine atoms are expected to be produced. However, when acetyl chloride was irradiated at 266 nm in a propane matrix, only the  $[\text{HCl}-\text{CH}_2\text{CO}]$  complex was formed; no products from the free chlorine atom were observed.
- (35) Goddard, W. A., III. *J. Am. Chem. Soc.* **1970**, *92*, 7520.
- (36) Goddard, W. A., III. *J. Am. Chem. Soc.* **1972**, *94*, 793.
- (37) Bock, H.; Takakuni, H.; Shamsheer, M.; Bahman, S. *Angew. Chem., Int. Ed. Engl.* **1977**, *16*, 105.
- (38) Sumathi, R.; Chandra, A. K. *Chem. Phys.* **1994**, *181*, 73.
- (39) Lennon, B. S.; Stimson, V. R. *J. Am. Chem. Soc.* **1969**, *91*, 7562.
- (40) Holbrook, K. A.; Marsh, A. R. W. *Trans. Faraday Soc.* **1967**, *63*, 643.
- (41) Choi, C. J.; Lee, B.-W.; Jung, K.-H.; Tschuikow-Roux, E. *J. Phys. Chem.* **1993**, *98*, 1139.
- (42) Stiefvater, O. L.; Wilson, E. B. *J. Chem. Phys.* **1969**, *50*, 5385.
- (43) Duncan, J. L.; Ferguson, A. M.; Harper, J.; Tonge, K. H. *J. Mol. Spectrosc.* **1987**, *125*, 196.
- (44) Moore, C. B.; Pimentel, G. C. *J. Chem. Phys.* **1963**, *38*, 2816.
- (45) Niiranen, J. K.; Gutman, D.; Krasnoperov, L. N. *J. Phys. Chem.* **1992**, *96*, 5881.
- (46) Gurvich, L. V.; Veyts, I. V.; Alcock, C. B.; Iorish, V. S. *Thermodynamic Properties of Individual Substances*, 4th ed.; Hemisphere: New York City, 1991; Vol. 2.
- (47) Nicovich, J. M.; Kreutter, K. D.; Wine, P. H. *J. Chem. Phys.* **1990**, *92*, 3639.
- (48) Berkowitz, J.; Ellison, G. B.; Gutman, D. *J. Phys. Chem.* **1994**, *98*, 2744.
- (49) Chase, M. W., Jr.; Davies, C. A.; Downey, J. R., Jr.; Frurip, D. J.; McDonald, R. A.; Syverud, A. N. JANAF Thermochemical Tables *J. Phys. Chem. Ref. Data* **1985**, *14* (Suppl. No. 1), 1.
- (50) Traeger, J. C.; McLoughlin, R. G.; Nicholson, A. J. *J. Am. Chem. Soc.* **1982**, *104*, 5318. Traeger et al. report the appearance potential for  $\text{CH}_3\text{CO}^+$  from acetaldehyde, acetone, and acetic acid:

reaction	AE/eV	$\Delta H_{\text{corr}}/\text{kJ mol}^{-1}$
$\text{CH}_3\text{CHO} \rightarrow \text{CH}_3\text{CO}^+ + \text{H} + \text{e}^-$	10.67	11.7
$\text{CH}_3\text{COCH}_3 \rightarrow \text{CH}_3\text{CO}^+ + \text{CH}_3 + \text{e}^-$	10.38	15.9
$\text{CH}_3\text{COOH} \rightarrow \text{CH}_3\text{CO}^+ + \text{OH} + \text{e}^-$	11.54	14.6

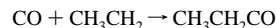
Using these values and the heats of formation given in Table 4, we calculated  $\Delta_f H(\text{CH}_3\text{CO}^+)$  at 0 and 298 K. For 298 K, we calculate  $156.7 \text{ kcal mol}^{-1}$ , while they report  $\Delta_f H_{298}(\text{CH}_3\text{CO}^+) = 657.0 \pm 1.5 \text{ kJ mol}^{-1} = 157.0 \pm 0.4 \text{ kcal mol}^{-1}$ . We defer to their value. Since we know  $\Delta_f H_0(\text{CH}_3\text{CO})$ , we can calculate the  $\text{IP}(\text{CH}_3\text{CO}) = 6.4 \pm 0.1 \text{ eV}$ .

(51) Holmes, J. L.; Lossing, F. P. *Int. J. Mass. Spectrom. Ion Processes* **1984**, *58*, 113. Holmes and Lossing report the appearance energy for  $\text{CH}_3\text{CH}_2^+$  formed from  $\text{CH}_3\text{CH}_2\text{COCl}$ :



We calculated  $\Delta_f H_0(\text{CH}_3\text{CH}_2\text{COCl})$  using  $\Delta_f H_0(\text{COCl})$  from Table 4 and  $\Delta_f H_0(\text{CH}_3\text{CH}_2^+) = 218.8 \pm 0.5 \text{ kcal mol}^{-1}$  (Berkowitz, J.; Ellison, G. B.; Gutman, D. *J. Phys. Chem.* **1994**, *98*, 2744).

(52) Watkins, K. W.; Thompson, W. W. *Int. J. Chem. Kinet.* **1973**, *5*, 791. Watkins and Thompson report  $\Delta_{\text{rxn}} H_{298} = -10.2 \pm 0.2 \text{ kcal mol}^{-1}$  and  $\Delta_{\text{rxn}} H_0 = -9.6 \pm 0.2 \text{ kcal mol}^{-1}$  for the reaction of CO with ethyl radical:

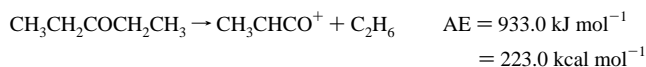


We calculated  $\Delta_f H(\text{CH}_3\text{CH}_2\text{CO})$  at 0 and 298 K using  $\Delta_f H(\text{CO})$  and  $\Delta_f H(\text{CH}_3\text{CH}_2)$  from Table 4. They report  $\Delta_f H_{298}(\text{CH}_3\text{CH}_2\text{CO}) = -10.6 \pm 1.0 \text{ kcal mol}^{-1}$  based on a value of  $\Delta_f H_{298}(\text{CH}_3\text{CH}_2) = 26 \text{ kcal mol}^{-1}$ .

(53) Ruscic, B.; Berkowitz, J.; Curtiss, L. A.; Pople, J. A. *J. Chem. Phys.* **1989**, *91*, 114.

(54) Seakins, P. W.; Pilling, M. J.; Niiranen, J. T.; Gutman, D.; Krasnoperov, L. N. *J. Phys. Chem.* **1992**, *96*, 9847.

(55) Traeger, J. C. *Org. Mass Spectrom.* **1985**, *20*, 223. Traeger reports an appearance potential for the formation of  $\text{CH}_3\text{CHCO}^+$  from  $\text{CH}_3\text{CH}_2\text{COCH}_2\text{CH}_3$ :



Using  $\Delta_f H_0(\text{CH}_3\text{CH}_2\text{COCH}_2\text{CH}_3)$  and  $\Delta_f H_0(\text{CH}_3\text{CH}_3)$  from Table 4 gives  $\Delta_f H_0(\text{CH}_3\text{CH}_2\text{CO}^+) = 186.1 \pm 2.5 \text{ kcal mol}^{-1}$ . Then, using the  $\text{IP}(\text{CH}_3\text{CHCO}) = 8.95 \text{ eV}$ , we compute  $\Delta_f H_0(\text{CH}_3\text{CHCO})$ .

(56) Aubry, C.; Holmes, J. L.; Terlouw, J. K. *J. Phys. Chem. A* **1997**, *101*, 5958.

(57) Wagman, D. D.; Evans, W. H.; Parker, V. B.; Schumm, R. H.; Halow, I.; Bailey, S. M.; Churney, K. L.; Nuttall, R. L. *The NBS tables of chemical thermodynamic properties*; National Bureau of Standards: Washington, DC, 1982; Vol. 11.

(58) Traeger, J. C. *Org. Mass Spectrom.* **1985**, *20*, 223. Traeger reports the appearance potential for  $\text{CH}_3\text{CH}_2\text{CO}^+$  from  $\text{CH}_3\text{CH}_2\text{CHO}$  and  $\text{CH}_3\text{-CH}_2\text{COCH}_3$ :

reaction	AE/eV	$\Delta H_{\text{corr}}/\text{kJ mol}^{-1}$
$\text{CH}_3\text{CH}_2\text{CHO} \rightarrow \text{CH}_3\text{CH}_2\text{CO}^+ + \text{H} + \text{e}^-$	10.18	14.5
$\text{CH}_3\text{CH}_2\text{COCH}_3 \rightarrow \text{CH}_3\text{CH}_2\text{CO}^+ + \text{CH}_3 + \text{e}^-$	9.90	18.7

Using these values and the heats of formation given in Table 4, we calculated  $\Delta_f H(\text{CH}_3\text{CH}_2\text{CO}^+)$  at 0 and 298 K. For 298 K, we calculate  $140.9 \text{ kcal mol}^{-1}$ , while Traeger reports  $\Delta_f H_{298}(\text{CH}_3\text{CH}_2\text{CO}^+) = 591.2 \pm 2.3 \text{ kJ mol}^{-1} = 141.3 \pm 0.5 \text{ kcal mol}^{-1}$ . We defer to this value. Since we know  $\Delta_f H_0(\text{CH}_3\text{CH}_2\text{CO})$ , we can calculate the  $\text{IP}(\text{CH}_3\text{CH}_2\text{CO}) = 6.8 \pm 0.1 \text{ eV}$ .

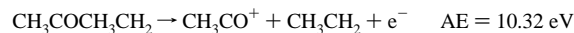
(59) Traeger, J. C. *Int. J. Mass Spectrom. Ion Processes* **1985**, *66*, 271. Traeger reports the appearance potential for  $\text{CHO}^+$  from  $\text{CH}_3\text{CH}_2\text{CHO}$ :



We determined  $\Delta_f H_0(\text{CHO}^+)$  from the  $\text{IP}(\text{CHO}) = 8.14 \pm 0.04 \text{ eV}$  and  $\Delta_f H_0(\text{CHO}) = 9.88 \pm 0.2 \text{ kcal mol}^{-1}$  (Berkowitz, J.; Ellison, G. B.; Gutman, D. *J. Phys. Chem.* **1994**, *98*, 2744).  $\Delta_f H_0(\text{CHO}^+) = 197.6 \pm 1.0 \text{ kcal mol}^{-1}$ .  $\Delta_f H_0(\text{CH}_3\text{CH}_2)$  from Table 4.

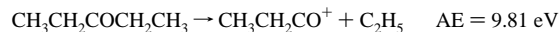
(60) Wiberg, K. B.; S., C. L.; Morgan, K. M. *J. Am. Chem. Soc.* **1991**, *113*, 3447.

(61) Traeger, J. C.; McLoughlin, R. G.; Nicholson, A. J. *J. Am. Chem. Soc.* **1982**, *104*, 5318. Traeger et al. report an appearance potential for  $\text{CH}_3\text{-CO}^+$  from  $\text{CH}_3\text{COCH}_3\text{CH}_2$ :



Using  $\Delta_f H_0(\text{CH}_3\text{CO}^+)$  and  $\Delta_f H_0(\text{CH}_3\text{CH}_2)$  from Table 4, we compute  $\Delta_f H_0(\text{CH}_3\text{COCH}_3\text{CH}_2)$ .

(62) Traeger, J. C. *Org. Mass Spectrom.* **1985**, *20*, 223. Traeger reports an appearance potential for the formation of  $\text{CH}_3\text{CH}_2\text{CO}^+$  from  $\text{CH}_3\text{CH}_2\text{-COCH}_2\text{CH}_3$ :



Using  $\Delta_f H_0(\text{CH}_3\text{CH}_2\text{CO}^+)$  and  $\Delta_f H_0(\text{C}_2\text{H}_5)$  from Table 4, we compute  $\Delta_f H_0(\text{CH}_3\text{CH}_2\text{COCH}_2\text{CH}_3)$ .